

Semi-insulating crystalline silicon formed by oxygen doping during low-temperature chemical vapor deposition

P. V. Schwartz,^{a)} C. W. Liu, and J. C. Sturm

Department of Electrical Engineering, Princeton University, Princeton, New Jersey 08544

(Received 22 October 1992; accepted for publication 4 January 1993)

In this letter we demonstrate the use of oxygen as a dopant in silicon to create semi-insulating, crystalline silicon films grown by chemical vapor deposition. The films contain oxygen concentrations that exceed the peak solid solubility of oxygen in silicon by several orders of magnitude, yet they remain crystalline. The resistivities of these films reach levels of $10^6 \Omega \text{ cm}$ at room temperature and the electronic properties of the films exhibit classical characteristics of space-charge-limited current associated with insulators containing trap states within the band gap. We then demonstrate that metal-oxide-semiconductor transistors with bulk-like mobilities can be fabricated in crystalline silicon layers grown without oxygen on top of the semi-insulating films.

Semi-insulating substrates are desirable for high-speed electronics because they provide circuits and devices with intrinsically low capacitances. One big advantage of III-V semiconductors over silicon for high-speed electronics is the availability of semi-insulating substrates. Previous work related to semi-insulating silicon layers resulted in the formation of semi-insulating polycrystalline silicon (SIPOS) films.¹ SIPOS films, which contain oxygen concentrations of a few tens of atomic percent, are used as part of passivation schemes for high-voltage semiconductor devices² as well as wide band-gap emitters in silicon-based heterojunction bipolar transistors (HBTs).³ Oxygen-doped silicon epitaxial films (OXSEF)⁴ were then introduced as a crystalline substitute for the wide band-gap material for silicon-based HBTs. The OXSEF layers are grown by molecular beam epitaxy in a temperature window of 300–700 °C.^{5,6} Even though the oxygen concentrations in the OXSEF films are on the order of a few tens of atomic percent, the films remain crystalline and when heavily doped with arsenic, they exhibit low resistivities. In this work, we continue the study of oxygen in crystalline silicon by introducing the oxygen as a dopant during low-temperature chemical vapor deposition of epitaxial silicon. It is known that oxygen creates energy levels within the silicon band gap at $E_v + 0.4 \text{ eV}$ and $E_v + 0.6 \text{ eV}$.⁷ By heavily doping the silicon films with oxygen, we attempt to pin the Fermi level near the silicon midgap and create a semi-insulating layer while maintaining the crystallinity of the epitaxial layer. The oxygen-doped silicon (Si:O) layers grown for this study contain oxygen concentrations on the order of 10^{20} cm^{-3} .

All epitaxial layers (both Si:O and pure Si) were grown in a susceptor-free, lamp-heated, chemical vapor deposition system described in detail elsewhere.⁸ The Si:O layers were grown on (100) silicon substrates that were chemically cleaned prior to loading into the reaction chamber. The wafers were then cleaned *in situ* at 1000 °C in a 250 Torr hydrogen ambient for 60 s. The system pressure

was then lowered to 6 Torr for growth of a 1.5 μm buffer layer using dichlorosilane as the silicon source gas. Following the buffer layer, the temperature was reduced to grow the Si:O layer (between 700 and 750 °C) and allowed to stabilize. At this point, silane (SiH_4) replaced DCS as the silicon source gas and the silane flow was also allowed to stabilize before the introduction of oxygen.

O_2 was chosen as the source gas for these experiments since it is easily removed from the growth environment as compared to water vapor which adsorbs to the quartz walls of the chamber. Since O_2 is readily removed from the growth environment, once the oxygen source is extinguished, its effects are not felt on subsequent layer growth. The oxygen was introduced to the growth environment in an argon carrier gas through a calibrated mass flow controller. The gas phase concentration of O_2 ranged from 5 ppm (parts per million) to 10 ppm while the oxygen concentrations in the epitaxial layers ranged from approximately 7×10^{19} – $1.4 \times 10^{20} \text{ cm}^{-3}$ at 750 °C and 1.8×10^{20} – $3.5 \times 10^{20} \text{ cm}^{-3}$ at 715 °C. We determined, by secondary ion mass spectrometry (SIMS), that the oxygen concentration in the epitaxial layer is proportional to the concentration of oxygen in the gas flow. This suggests that we have entered a low-temperature kinetic limit for oxygen incorporation in the epitaxial layer. The epitaxial films grown at low temperature exhibit specular reflection of light with no signs of haze on the wafer surface, even with an oxygen concentration of 10^{20} cm^{-3} .

We studied the characteristics of Si:O layers using Fourier transform infrared (FTIR) spectroscopy transmission measurements. Figure 1 shows a transmission spectrum of a 5 μm thick film of Si:O doped with oxygen to a level of $\sim 10^{20} \text{ cm}^{-3}$ on a float zone substrate normalized to a substrate without an epitaxial layer so that the absorption spectrum contains negligible contributions from the oxygen in substrate. Arrows on the figure mark the vibrational energies for the Si—O bond when oxygen takes the form of an interstitial atom (1107 cm^{-1}) and SiO_2 precipitates (1100 – 1230 cm^{-1}). Notice that the absorption peak in the Si:O is shifted to an energy lower than that of the interstitial oxygen and has a full width at half maximum

^{a)}Present address: Department of Electrical and Computer Engineering, University of Iowa, Iowa City, IA 52242.

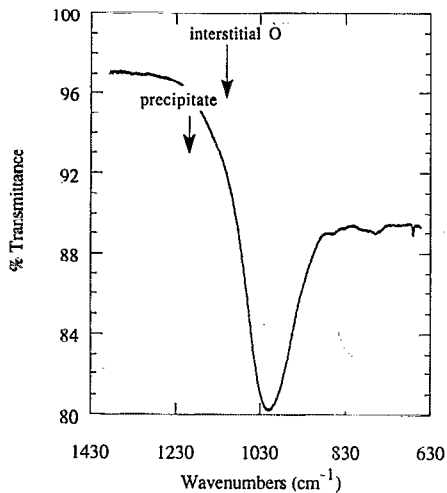


FIG. 1. FTIR transmission spectrum of a 5 μm thick sample of Si:O doped with oxygen to $\sim 10^{20} \text{ cm}^{-3}$. The arrows denote the vibrational energies for interstitial oxygen (1107 cm^{-1}) and SiO_2 precipitates ($1100\text{--}1230 \text{ cm}^{-1}$). Note the peak shift away from the interstitial peak to a lower energy for the Si:O layer.

(FWHM) much larger than the accepted value of 32 cm^{-1} associated with interstitial oxygen. This broadened and shifted peak is similar to the spectra seen for OXSEF as reported by Tabe *et al.*⁶ We cannot make a positive determination of the oxygen configuration in the silicon lattice, but the data are not consistent with the classical formation of SiO_2 precipitates because of the peak shift to lower energies. Tabe *et al.* explained this shift by the formation of $\text{SiO}_{1.5}$ instead of the complete phase separation into SiO_2 precipitates. With SiO_2 precipitates, the emergence of absorption lines is typically seen at energies higher than the interstitial energy.¹¹

Even though these layers contain oxygen concentrations exceeding the peak solid solubility for interstitial oxygen in silicon, the layers remain crystalline. We studied the crystallinity of the layers by x-ray diffraction techniques. A diffraction spectrum for a 5 μm thick Si:O layer containing $5 \times 10^{19} \text{ cm}^{-3}$ of oxygen is shown in Fig. 2. Note that the intensity scale is logarithmic. In this spectrum, we see only peaks associated with (100) crystalline silicon demonstrating the crystalline nature of the films. (The system filter was not able to resolve the α and β source lines.)

We characterized the electronic properties of the Si:O films by fabricating a variety of devices. Initial resistivity measurements were made using Schottky diodes formed by evaporating aluminum directly on the Si:O layer. We chose to measure vertical transport of carriers to avoid parallel conduction paths through the silicon substrate. Figure 3 is an Arrhenius plot of the Si:O resistivity of two films doped $\sim 5 \times 10^{19}$ and $2 \times 10^{20} \text{ cm}^{-3}$ with oxygen, both films are 10 μm thick and have device areas of 0.0018 cm^2 . Note that the room-temperature resistivities of the films reach $10^6 \Omega \text{ cm}$. The resistivity measurements were made with a forward bias of 4 V to ensure that we measured the film characteristics and not the resistance of the Schottky barrier. The reverse bias currents were several orders of mag-

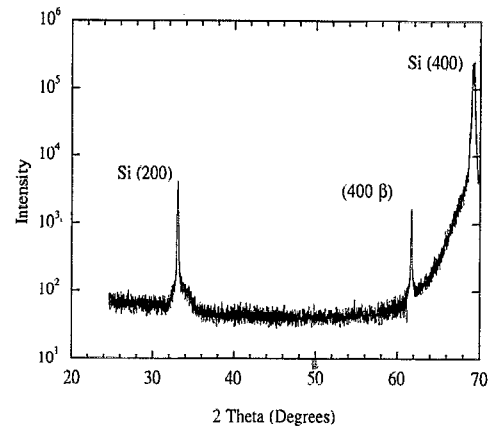


FIG. 2. X-ray diffraction spectrum for a Si:O layer doped $\sim 5 \times 10^{19} \text{ cm}^{-3}$ with oxygen. We see only peaks associated with (100) crystalline silicon for $\text{Cu } K_\alpha$ and $\text{Cu } K_\beta$ radiation. If polycrystalline silicon were present, a dominant peak at $2\theta = 28^\circ$ would appear.

nitude lower than the forward bias currents. From the activation energy of the plot, we determine that the Fermi level is pinned at either $E_c - 0.6 \text{ eV}$ or $E_v + 0.6 \text{ eV}$, which is very close to midgap.

The oxygen-doped layers also demonstrate classic characteristics of space-charge-limited current for insulating materials containing energy levels within the band gap as is evident from Fig. 4. Figure 4 shows a logarithmic plot of the current and voltage for a (*p*-Si)-Si:O-(*p*-Si) structure. Here we give a physical picture of space-charge-limited current in insulators which contain background thermal carriers and trap levels within the band gap according to the theory of Lampert and Mark,⁹ and we discuss the current-voltage relationship in such materials.

As a bias is applied to such a material, carriers are injected into the insulator and they contribute to space charge. Until the injected carrier concentration exceeds the background concentration, however, the charge of the injected carriers has little effect on the electric field or con-

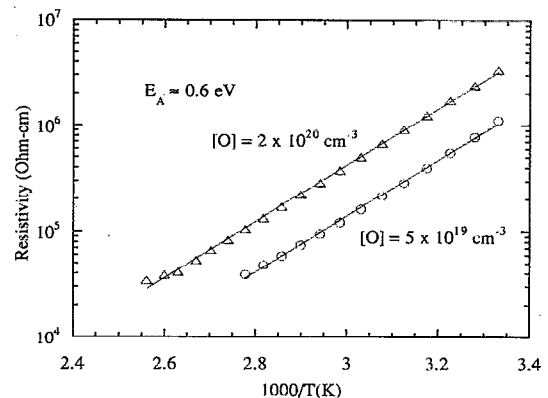


FIG. 3. Resistivity of Si:O Schottky diodes as a function of inverse temperature. One film is doped $\sim 5 \times 10^{19} \text{ cm}^{-3}$ and the other $\sim 2 \times 10^{20} \text{ cm}^{-3}$ with oxygen. The room-temperature resistivities of both films reach $10^6 \Omega \text{ cm}$ and the activation energies are $\sim 0.6 \text{ eV}$. The film thickness is 10 μm and the device areas are 0.0018 cm^2 . The resistivity measurements were taken at 4 V forward bias.

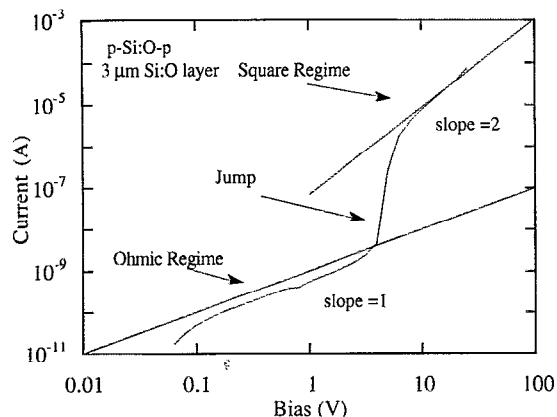


FIG. 4. Logarithm of current and voltage for a (*p*-Si)-Si:O-(*p*-Si) diode with a Si:O layer thickness of 3 μm . The three current regimes correspond to the low bias regime where current is dominated by background carriers (slope of one), the sudden increase in current with voltage corresponding to the filling of trap levels (jump) and the square law regime where space-charge dominates (slope of two).

ductivity and Ohm's law is obeyed. This corresponds to a slope of one on the logarithmic plot of current and voltage in Fig. 4. (The data of Fig. 3 are taken in this regime.) Initially the injected carriers also serve to fill the empty trap levels within the insulator band gap. Once all of the trap sites are filled, the Fermi level is allowed to move away from the trap level and the current increases sharply with a small increase in voltage. In Fig. 4, this corresponds to the region labeled jump. Once the traps are filled and the injected carrier concentration exceeds the thermal concentration, the space charge established by the injected carriers dominates the electric field and hence the voltage drop. Current flow in a space-charge-limited regime is proportional to the square of the applied bias ($J \propto V^2$). This corresponds to the region exhibiting a slope of two in Fig. 4. The existence of the large jump in the current with a small increase in voltage demonstrates the high concentration of traps within the band gap as expected. The ratio of the density of filled traps to empty traps in the material is given by the magnitude of the current jump. From the jump in current of Fig. 4 and the estimated background carrier concentration (in pure silicon grown in our reactor at 750 $^\circ\text{C}$) of 10^{16} cm^{-3} , we estimate the total number of traps in this Si:O layer to be $\sim 10^{19} \text{ cm}^{-3}$. We find that we can saturate these trap levels by heavily doping the films, either *n*- or *p*-type, such that the films conduct. This is consistent with heavy doping results of OXSEF⁴ and unintentionally oxygen-doped Si_{1-x}Ge_x layers.¹¹

We now demonstrate exploiting the semi-insulating and crystalline features of the Si:O as a semi-insulating substrate on which to directly grow crystalline silicon.

We fabricated MOS transistors in the crystalline silicon grown directly upon a 1.5 μm thick Si:O layer (grown at 750 $^\circ\text{C}$). The capping layers of pure silicon (forming active regions for the devices) were grown at 1000 $^\circ\text{C}$ without oxygen following the growth of the Si:O layer. We fabricated *p*-MOS transistors with gate lengths ranging from 2 to 50 μm using a self-aligned process. Device iso-

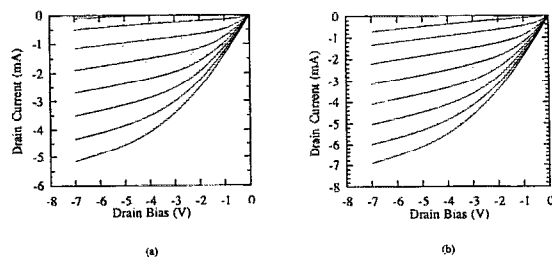


FIG. 5. Current-voltage characteristic of (a) a *p*-MOS transistor fabricated in undoped silicon grown directly on a 1.5 μm thick layer of Si:O, and (b) a *p*-MOS transistor fabricated in a virgin silicon wafer. The characteristics show that the carrier mobility in the Si:O device is similar to the virgin silicon demonstrating that the active area of the Si:O transistor is of device quality. Voltage steps = 1 V.

lation was provided by mesa etching the active area of the devices. The *I-V* characteristics of a 2 μm gate *p*-MOS transistor fabricated in silicon-on-Si:O are shown in Fig. 5 along with an identical structure fabricated in a bulk silicon wafer processed in parallel with the silicon-on-Si:O devices. The two devices exhibit similar characteristics demonstrating that the silicon forming the active region of the Si:O structure has a mobility similar to that in virgin silicon substrates. Work is currently underway to further investigate the crystalline and semi-insulating properties of the oxygen-doped silicon layers and lifetimes in the overlying silicon layers.

In conclusion, we determined that one can pin the Fermi-level near midgap in silicon with the introduction of large amounts of oxygen in the silicon lattice during low-temperature CVD, yet we can still maintain the crystalline structure. We also showed that device quality crystalline silicon can be grown directly upon the semi-insulating layer. This work was supported by ONR (No. N00014-90-J1316) and NSF (No. ECS-8657227). The authors would like to thank G. Dolny of David Sarnoff Research Center for poly-silicon deposition.

¹H. Mochizuki, T. Aoki, H. Yamoto, M. Okayama, and T. Ando, Suppl. Jpn. J. Appl. Phys. **15**, 41 (1976).

²T. Matsushita, T. Aoki, T. Ohtsu, H. Yamoto, H. Yayashi, M. Okayama, and Y. Kawana, IEEE Trans. Electron Devices **TED-23**, 826 (1976).

³T. Matsushita, N. Oh-uchi, H. Hayashi, and H. Yamoto, Appl. Phys. Lett. **35**, 549 (1979).

⁴M. Takahishi, M. Tabe, and Y. Sakakibara, IEEE Electron Device Lett. **EDL-8** 475 (1987).

⁵T. J. Mahoney, J. Vac. Sci. Technol. **B 1**, 773 (1983).

⁶M. Tabe, M. Takahashi, and Y. Sakakibara, Jpn. J. Appl. Phys. **26**, 1830 (1987).

⁷S. M. Sze, *Physics of Semiconductor Devices*, 2nd ed. (Wiley, New York, 1981), p. 27.

⁸J. C. Sturm, P. V. Schwartz, and E. J. Prinz, J. Vac. Sci. Technol. **B 9**, 2011 (1991).

⁹M. A. Lampert and P. Mark, *Current Injection In Solids* (Academic, New York, 1970).